

High WTAP expression level as a promising biomarker for poor prognosis in colorectal cancer: a pilot study

Michela Relucenti,¹ Claudia Tito,² Paolo Mercantini,³ Emanuela Pillozzi,⁴ Claudio Barbaranelli,⁵ Loredana Cristiano,¹ Daniela Savarese,⁶ Daniela Bastianelli,⁶ Francesco Fazi,² Vincenzo Petrozza,⁶ Xiaobo Li,⁷ Rui Chen,⁷ Selenia Miglicetta,^{1*} Giuseppe Familiari^{1*}

¹Department of Anatomical, Histological, Forensic, and Orthopaedic Sciences, Section of Anatomy, Sapienza University of Rome, Italy; ²Department of Anatomical, Histological, Forensic, and Orthopaedic Sciences, Section of Histology and Medical Embryology, Sapienza University of Rome, Italy; ³Surgery Unit, Department of Medical Surgical Sciences and Translational Medicine, Sapienza University of Rome, Sant'Andrea University Hospital, Rome, Italy; ⁴Pathology Unit, Department of Clinical and Molecular Medicine, Sapienza University of Rome, Sant'Andrea University Hospital, Rome, Italy; ⁵Psychology Department, Sapienza University, Rome, Italy; ⁶Department of Medico-Surgical Sciences and Biotechnologies, Sapienza University of Rome, Pathology Unit ICOT, Latina, Italy; ⁷Key Laboratory of Environmental Medicine Engineering, Ministry of Education, School of Public Health, Southeast University, Nanjing, China

*These authors contributed equally

ABSTRACT

Colorectal cancer (CRC) is a major public health concern and identifying prognostic molecular biomarkers can help stratify patients based on risk profiles, thus enabling personalized medicine. Epitranscriptomic modifications play a relevant role in controlling gene expression, N6-methyladenosine (m6A) regulators play crucial roles in cancer progression, but their clinical significance in CRC cancer has thus far not been elucidated. Thus, we aimed to examine by immunohistochemical techniques and RT-qPCR, protein levels and RNAs expression of m6A writers (METTL3, WTAP) and eraser (FTO) in a cohort of 10 patients affected by CRC. The patients were followed for 5 years and values of METTL3, WTAP and FTO RNAs in alive vs dead patients were compared. Proteins expression and RNAs expression had a different trend, METTL3, WTAP and FTO proteins' expression showed an increasing trend from non-cancerous adjacent (N) tissue vs carcinoma (CA) tissue G1 stage, and then a decreasing trend from G1 to G2 and G3 stages. The most marked increase was observed in WTAP that, from a 40% of protein expression positivity in N tissue raised to the 81% of positivity in G1 stage K tissue. RNAs expression of METTL3, WTAP and FTO genes in N tissue vs G1 stage CA tissue was significantly different, the analysis and comparison of RNAs values in patient alive after 5 years (0.58 ± 0.04) vs patients dead after 5 years (1.69 ± 0.29) showed that only WTAP values resulted significantly high in dead patients. The fact that WTAP protein expression levels lower while WTAP RNA expression remains high, let us hypothesize a sort of inhibition of protein expression, but further studies are needed to clarify the mechanism. Although the results suggest a relationship between biological meaning and prognostic utility of WTAP, this prognostic utility must be confirmed by further studies on a larger sample.

Key words: colorectal cancer; METTL3; WTAP; FTO; biomarkers.

Correspondence: Michela Relucenti, Department of Anatomical, Histological, Forensic, and Orthopaedic Sciences, Section of Anatomy, Sapienza University of Rome, via Alfonso Borelli 50, 00161 Rome, Italy.
E-mail: michela.relucenti@uniroma1.it

Contribution: all authors have contributed significantly, and all authors agree with the content of the manuscript.

Conflict of interest: the authors declare no competing interests.

Ethics approval: this pilot study was approved by the Institutional Review Board of the Sapienza University of Rome, Italy (no. RS5304/2019).

Availability of data and materials: the data used to support the findings of this study are available from the corresponding author upon reasonable request.

Funding: the present study was supported by grants from Sostituire con Donazione Ecorad 2024.

Introduction

Colorectal cancer (CRC) is a prevalent malignancy affecting the colon or the rectum, representing the third most common cancer worldwide. In Europe, in 2020, CRC was estimated to be the second most diagnosed cancer and the second leading cause of cancer death.¹ Although early CRC detection reduces patients' mortality² and there are significant advancements in diagnostic techniques and treatment approaches, the clinical outlook for CRC individuals remains unsatisfactory due to the advanced stage at the time of diagnosis, when cancer invades secondary organs, such as the liver.³ The limits of current non-invasive diagnostic screening that are not sensitive to detect pre-cancerous lesions and difficulty in establishing appropriate surrogate markers for early disease detection driven researchers to find new prognostic biomarkers to predict disease progression including early recurrence and mortality.

Currently, only *KRAS*, *NRAS*, *BRAF*, and MSI status are recommended by national guidelines in evaluating treatment response and predicting outcomes in CRC.⁴⁻⁷

In a modern view of personalized medicine, molecular biomarkers with a possible prognostic value are needed to guide clinicians in tailoring therapies based on the specific biological features of the tumor. Hence, a thorough investigation into the molecular biology of CRC is essential to identify new biomarkers for the prognosis of CRC progression. Since cancer tissues showed different gene expression profiles compared to regular counterparts, the study of gene expression regulation in cancer has been well investigated. In this context, epitranscriptomic modifications are relevant in controlling gene expression.^{8,9} In particular, the N6-methyladenosine (m6A) modification represents one of the most widespread epigenetic methylations of both mRNAs and noncoding RNAs (ncRNAs),¹⁰⁻¹² affecting significantly various aspects of RNA, including translation, splicing, transport, and stability.^{13,14} Several studies revealed that the abnormal methylation of m6A is associated with different types of cancers¹⁵ suggesting its crucial role in the tumorigenesis process.¹⁶⁻¹⁸ m6A modification is performed by other enzymes, including methyltransferases, RNA-binding proteins, and demethylases.¹⁹ Methyltransferases catalyze RNA m6A modification, and they are composed of several proteins like METTL3 (methyltransferase like 3) and WTAP (Wilms tumor1 associating protein); on the contrary, demethylases remove m6A modification of RNA and they include FTO (fat mass and obesity-associated protein) which is the first m6A demethylase discovered; finally, RNA-binding proteins bind RNA and regulate gene expression. Considering their functional activity, methyltransferases are called "writers," demethylases "erasers," and RNA-binding proteins "readers".^{20,21} To find possible new molecular biomarkers for CRC prognosis, we investigated the mRNA and protein expression of m6A writers (METTL3, WTAP) and eraser (FTO) in a group of 10 CRC patients, comparing protein expression levels in normal-adjacent tissues vs G1-G3 CRC tissues and examining RNAs expression between adjacent non-cancerous tissues and CRC tissues, comparing then their values, after 5 years, in patients who were still living and those who had died.

Materials and Methods

Ethics statement

This pilot study was approved by the Institutional Review

Board of the Sapienza University of Rome (RS5304/2019) and conducted according to good clinical practice and the ethics of the Helsinki Declaration.

Patients' characteristics and sample collection

Adjacent non-cancerous tissue and corresponding different grades (G1, G2, and G3) of tumoral tissue were retrieved from a cohort of 10 patients (5 women, and 5 men, older than 56 years), affected by CRC at different stages (I-IV), according to the Tumor Nodes Metastasis (TNM) staging system and Tumor grades (G1-G3) subjected to surgery at Sant'Andrea Hospital in Rome from May 2018 to July 2020. Table 1 reports each patient's colon cancer location, TNM staging, and tumor grade.

The histological subtype and tumor grade assignment were based on the percentage of glandular structure formation in the tumor area according to WHO classification:¹⁹ grade G1 >95%, grade G2 50-95%, grade G3 0-49%, G4-no gland formation.

According to WHO recommendations, all the examined samples belonged to grades G1-G3; G1-G2 were considered tumors with low malignancy, and G3-G4 were considered with a high degree of malignancy.²²⁻²⁴

Patients with a newly histologically confirmed diagnosis of primary colon neoplasm cancer (by an expert pathologist (E.P.) of the Pathology Lab of Sant'Andrea Hospital), who underwent laparoscopic resection surgery with curative intent, were eligible. The exclusion criteria adopted were pregnancy, relapsing cancer or metastatic cancer, simultaneous diagnosis of other neoplasms, cancer treatment in the five years before recruitment, severe cardiovascular, pulmonary, orthopedic, and neurological pathologies, cognitive impairment, and regular use of immunosuppressive drugs. The study was explained in detail during the assessment, and the inclusion and exclusion criteria were evaluated. Eligible patients who agreed to participate signed written informed consent. The list of 5-year survived and dead patients with respective tumor locations, TNM, and tumor grades are reported in Table 2.

Histopathological procedures

Colon carcinoma specimens were fixed in 3,7% formalin (Bio-Optica, Milan, Italy) for 48 h, at room temperature, dehydrated in the ascending series of alcohol, dipped in xylene, embedded in paraffin blocks, and cut with a microtome (RM2255; Leica, Wetzlar, Germany) into 2 µm thick serial sections. Sections were then deparaffined and hydrated through xylenes and a descending series of alcohol, stained with Hematoxylin and Eosin (H&E) according to the manufacturer's instruction (Bio Optica) and observed by light microscopy (microscope Axioskop 40; Zeiss, Göttingen, Germany) for morphological evaluations.

Immunohistochemistry

Deparaffinized sections were boiled in 10 mM citrate buffer, pH 6.1 (Bio-Optica) in a microwave at 720 W (3 cycles/3 min each) for antigen retrieval. The sections were then subjected to treatment for blocking endogenous peroxidase activity (Dako, Glostrup, Denmark). After thorough washing, sections of each sample were incubated, overnight at 4°C, with M.O.M rabbit IgG blocking reagent (Vector Laboratories, Newark, CA, USA) according to the manufacturer's protocol. Later sections were incubated with rabbit polyclonal primary antibodies, anti-FTO, anti-METTL3, or anti-WTAP, (Proteintech, Planegg-Martinsried, Germany) diluted 1:200 in M.O.M diluent for 30 min, according to the Vector Laboratories instructions. Primary antibodies were then revealed by biotinylated anti-rabbit IgG, followed by streptavidin-horse-radish peroxidase (HRP), 3,3-diaminobenzidine (DAB) substrate

buffer, and DAB (Dako kit, Santa Clara, CA, USA), according to manufacturer's instructions.²⁵ Negative controls were performed by omitting the primary antibody and substituting it with M.O.M diluent alone. Sections were counterstained with hematoxylin (Bio-Optica). Finally, three different sections for each sample were dehydrated and mounted with Neomount (Merck, Darmstadt, Germany). Twenty microscopic fields for each section were observed by a 40x objective, and photographed under the Zeiss microscope Axioskop 40, equipped with a Zeiss AxioCamMRc digital camera (Zeiss). The percentage of positivity to examined markers was obtained by recording the positive cells/total cell nuclei ratio.

Light and transmission electron microscopy procedures

Samples were prepared according to this procedure: fixation in 2.5% glutaraldehyde (Electron Microscopy Sciences, EMS, Hatfield, PA, USA) in Phosphate buffer 0.1M pH 7.4, for at least 48 h, at 4°C; post-fixation in osmium tetroxide 1.33% in dH₂O (Agar Scientific, Stansted, UK), for 2 h; dehydration in ascending alcohol series; propylene oxide (Sigma-Aldrich, St. Louis, MO, USA) for 40 min; 1:1 solution of propylene oxide/epoxy resin (Agar Scientific); overnight epoxy resin embedding and polymerization in a stove for 48 h at 60°C.

Resin blocks were cut with a diamond knife in semithin (1 µm thick, for light microscopy) and ultrathin (90-100 nm thick) sections using an Ultracut E ultramicrotome (EMUC6, Leica). Semithin sections were stained with methylene blue (Sigma-Aldrich) and photographed with the Zeiss Axioskop 40 microscope. Digital images were acquired by the Zeiss AxioCamMRc camera. Ultrathin sections were mounted on 100-mesh copper grids (Assing, Rome, Italy), contrasted using Uranylless (Uranyl acetate alternative) (TAAB Laboratories Equipment Ltd., Aldermaston, UK) and lead citrate (Electron Microscopy Sciences) and analyzed using a TEM (EM10, Zeiss, Oberkochen, Germany), operating at 60 kV. Images were acquired using a digital camera (AMT CCD, Deben UK Ltd., Suffolk, UK).²⁶⁻³⁰

Molecular characterization of samples: RNA extraction and RNA expression analysis

Fresh frozen samples were homogenized by a gentle dissociator (Miltenyi Biotec, Bergisch Gladbach, Germany) in 700 µL of Qiazol (Qiagen, Chatsworth, CA) and RNA was extracted following the manufacturer's instruction. The concentration and purity of total RNA were assessed using a Nanodrop TM 1000 spectrophotometer (Nanodrop Technologies, Wilmington, DE, USA). A quantity of 250 ng of total RNA was reverse transcribed using High-Capacity RNA-to-cDNA Kit (Applied Biosystems, Carlsbad, CA, USA) and diluted 1:5 for Quantitative Real-time PCR (RT-qPCR) experiments. Quantification of gene expression was measured by Sybr Green assay (Applied Biosystems) on Abi Prism 7500 Sequence Detection System (Applied Biosystems), using the following primers:

WTAP (FW: 5'-GGCGAAGTGTCGAAT GCT-3'; RW: 5'-CCAAGTCTGGCGTGTCT-3'); METTL3 (FW: 5'-AAGCAGCTGGACTCTCTGCG-3'; RW: 5'-GCA CTGGCT-GTCAC-TACGG-3'); FTO (FW: 5'-TGGGTTTCATCCTA-CAACGG-3'; RW: 5'-CCTCTTCAGGGCCTTCAC-3').

Gene expression levels were analyzed by absolute quantification method relative to a standard curve; the standard curve was performed with serial dilution of a reference cDNA obtained from RNA extracted from a tumor sample. All reactions were performed in duplicate.

Statistical analyses

Molecular data were statistically evaluated by the software by MedCalc[®] software (version 20.218, MedCalc Software Ltd., Ostend, Belgium) and SPSS[®] statistical software (version 29, IBM[®], Milan, Italy). The statistical analysis of immunohistochemical data, expressed as mean ±SD was calculated using a paired parametric *t*-test for matched samples. The statistical analysis of *METTL3*, *WTAP*, and *FTO* gene expression data, evaluated by RT-qPCR, using the paired parametric *t*-test for matched samples and the bootstrap estimation of the confidence interval (Cohen's *d* effects size).³¹ Differences in values were considered significant at *p*<0.05.

Results

Histopathological observations

Representative images of adjacent non-cancerous and cancerous colorectal tissue are represented in Figure 1 by hematoxylin-eosin (A-D) and methylene blue (E-H) staining. Ultrastructural analysis of ultrathin sections to transmission electron microscopy is also reported (Figure 1 I-N).

Compared to adjacent non-cancerous colonic mucosa (Figure 1A), tumoral tissues showed an altered architecture characterized by shorter and coiled glandular structures in the G1 and G2 stages (Figure 1 B,C) that remained as scattered glands remnants and displayed a spheroidal shape in G3 stage (Figure 1D). In addition, whereas the adjacent non-cancerous colonic mucosa showed well-differentiated enterocytes and goblet cells ordinally arranged in a monolayer (Figure 1E) the G1 sample displayed a tortuous structure of colonic glands, enterocytes, and goblet cells with heterogeneous shapes: taller and thinner cells, shorter and larger cells, apoptotic and necrotic cells, and capillary vessels (Figure 1F). Severely altered colonic gland structures characterized by different intensities of connective tissue in the lamina propria associated with an increased number of apoptotic and necrotic cells are shown in the G2 sample. Moreover, enterocytes were poorly differentiated, with large nuclei showing chromatin patches (Figure 1G). More alteration is shown in the G3 stage. The glandular structures were almost in-distinct, characterized by a few scattered remnants of still differentiated enterocytes dispersed in a context of undifferentiated round cells with large nuclei. Large and irregular capillary vessels are often detected (Figure 1H). Details of the enterocytes and goblet cells' ultrastructure to electron microscopy showed that well-differentiated enterocytes exhibit preserved junctional complexes and microvilli. In addition, the enterocyte borders a goblet cell in the right corner of the image (Figure 1I). Enterocytes in the G1 stage, although still well-differentiated and in tight contact with each other, showed irregular nuclei and enlarged endoplasmic reticulum (Figure 1L). Enterocytes in the G2 stage appeared as heterogeneous cells with a cubic/round shape rather than columnar and irregular microvilli that often lack polarity. Irregular nuclei and large cytoplasmic vacuoles are present (Figure 1M). Finally, enterocytes in the G3 stage were characterized by numerous undifferentiated round cells that lost contact with neighboring cells. Their cytoplasm is rich in mitochondria, and their nuclei show chromatin patches. Although the undifferentiated cells were more abundant than differentiated ones, the latter were still recognizable as enterocytes (Figure 1N).

Immunohistochemical results

METTL3, WTAP, and FTO protein expression revealed by immunohistochemical staining are represented in Figures 2 and 3. The immunohistochemical staining for METTL3 (Figure 2 A-D) demonstrated that the protein, localized in the nucleus and cytoplasm was expressed in adjacent non-cancerous tissue. The protein level increases in G1, remains quite stable in G2 and declines in G3 tissue. In addition, in G1 and G2 the protein has a localization strongly nuclear and cytoplasmic whereas in G3 becomes perinuclear in some cells and predominantly cytoplasmic in all tissue cells tissue. WTAP staining (Figure 2 E-H) indicated that the protein was expressed at deficient levels (40%) in adjacent non-cancerous tissue with cytoplasmic localization. Protein expression strongly increases in G1 (81%), localizing in the nucleus, then it declines in G2 and slightly in G3 stages. Finally, FTO staining (Figure 2 I-N) showed that the protein with almost mainly nuclear localization in adjacent non-cancerous tissue increases in colorec-

tal G1 tumor grade exhibiting a nuclear and cytoplasmic localization and then decreases in G2 tumor grade (M) in G3 tissues, changing its localization from nuclear to more cytoplasmic. To clarify even more the pattern of expression of METTL3, WTAP, and FTO as a function of the degree of malignancy, we have graphically depicted the percent cell positivity for each of the three markers (Figure 3), values obtained from analysis of immunohistochemical images in Figure 2. It can be seen from the graph that METTL3 value increases from adjacent non-tumoral tissue to G1 grade tissue, declines slightly in G2, and then declines again in G3. WTAP shows a marked difference in expression between adjacent non-tumoral tissue and G1 grade tissue, its expression then drops slightly in G2 and then again in G3. FTO value increases slightly from adjacent non-tumoral tissue to G1 grade tissue, increases again in G2, and then declines in G3. A statistical analysis of these data was not performed because the sample of patients for each tumor grade was too small (Table 1).

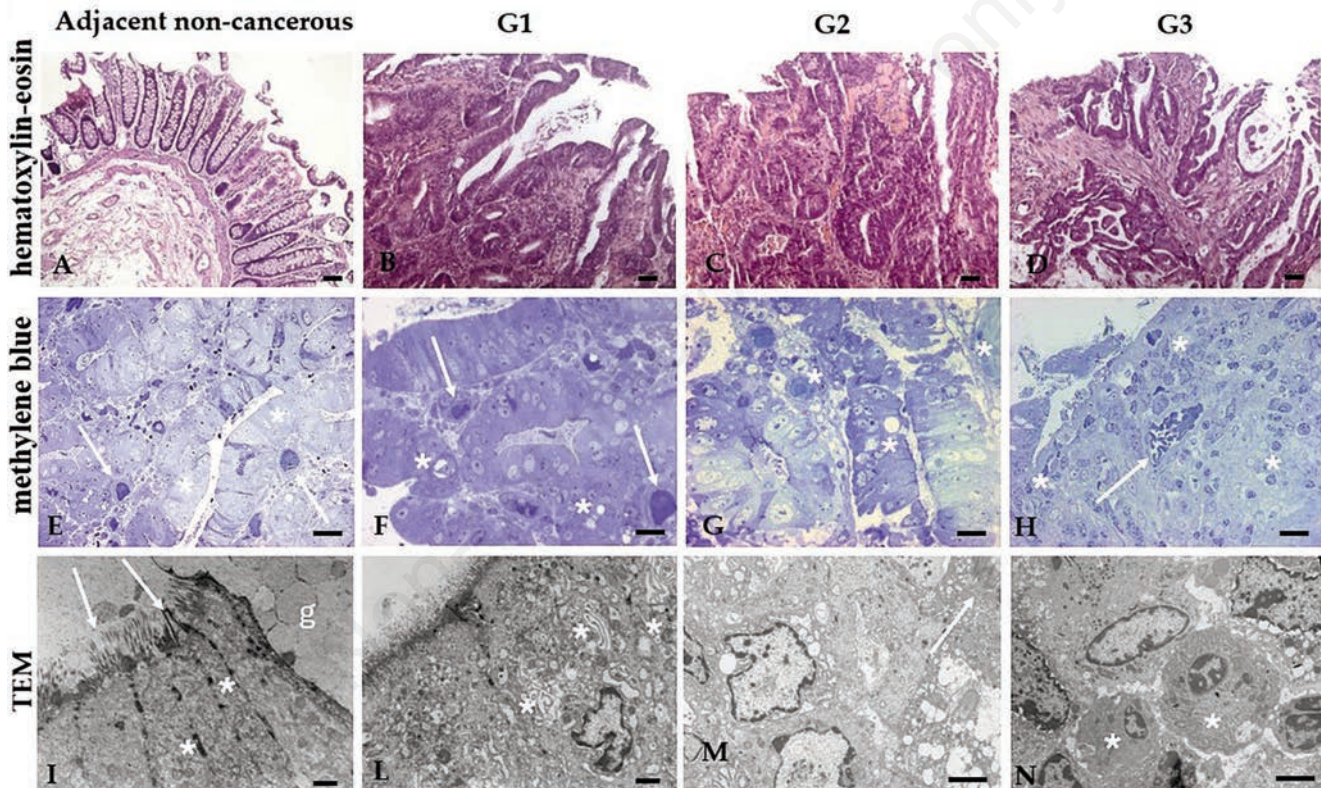


Figure 1. Histological analyses of adjacent non-cancerous and cancerous tissue in patients with different tumor grades (G1, G2, and G3). **A-D)** H&E staining, scale bar: 50 μ m. **A)** adjacent non-cancerous mucosa with well-developed glands. **B)** G1 stage colonic mucosa with moderately altered glands. **C)** G2 stage with severely altered glands. **D)** G3 stage colonic mucosa, colonic glands are virtually unrecognizable. **E-H)** Semithin sections stained with methylene blue, scale bar: 50 μ m. **E)** in the normal colonic mucosa, the epithelium presents enterocytes, goblet cells ordinately arranged (asterisk), and the submucosa well vascularized (arrows). **F)** The colonic epithelium exhibits an irregular layer due to the heterogeneous shape of enterocytes; taller and thinner cells are inter-mingled with shorter and larger cells, and some apoptotic and necrotic cells are visible (asterisks); the submucosa is richly vascularized (arrows). **G)** A severely altered colonic gland structure characterizes the G2 sample; numerous apoptotic and necrotic cells (asterisks) are visible; less differentiated enterocytes with large nuclei showing chromatin patches are present. **H)** In the G3 stage, no clear distinction between epithelium and submucosa is evident; glandular structures are almost unrecognizable; most cells are undifferentiated (asterisks); capillary vessels are more prominent and irregular (arrow). **I-N)** transmission electron microscopy images; scale bars: I,L) 1 μ m, M,N) 2 μ m. **I)** Enterocytes with intact junctional complexes (asterisks) and microvilli (arrows) and a goblet cell (g) are illustrated. **L)** G1 stage enterocytes are still well-differentiated, maintaining intercellular contact; nuclei are irregular, and the endoplasmic reticulum (asterisks) is enlarged. **M)** Enterocytes in G2 have cubic/spherical shapes rather than columnar; often, they lack polarity, showing few microvilli (arrow); irregular nuclei and large cytoplasmic vacuoles (asterisks) are present. **N)** Undifferentiated round cells (asterisks) characterize the G3 stage; their cytoplasm is rich in mitochondria and nuclei show chromatin patches; these cells lose contact with neighbor cells.

Writers and erasers RNAs expression

The expressions of METTL3, WTAP, and FTO RNAs, has been evaluated by RT-qPCR in adjacent non-cancerous (N) and carcinoma (CA) tissue, results are illustrated in Figure 4. Results demonstrated that all the markers were significantly more

expressed ($p < 0.05$) in colon carcinoma tissue. Statistical data analysis was performed firstly by summary statistics and then, being the distributions normal according to D'Agostino Pearson test, using parametric *t*-test, detailed results are reported in the caption of Figure 4. The data were also confirmed using the bootstrap estimation of the confidence interval. Cohen's *d* values of 1.418

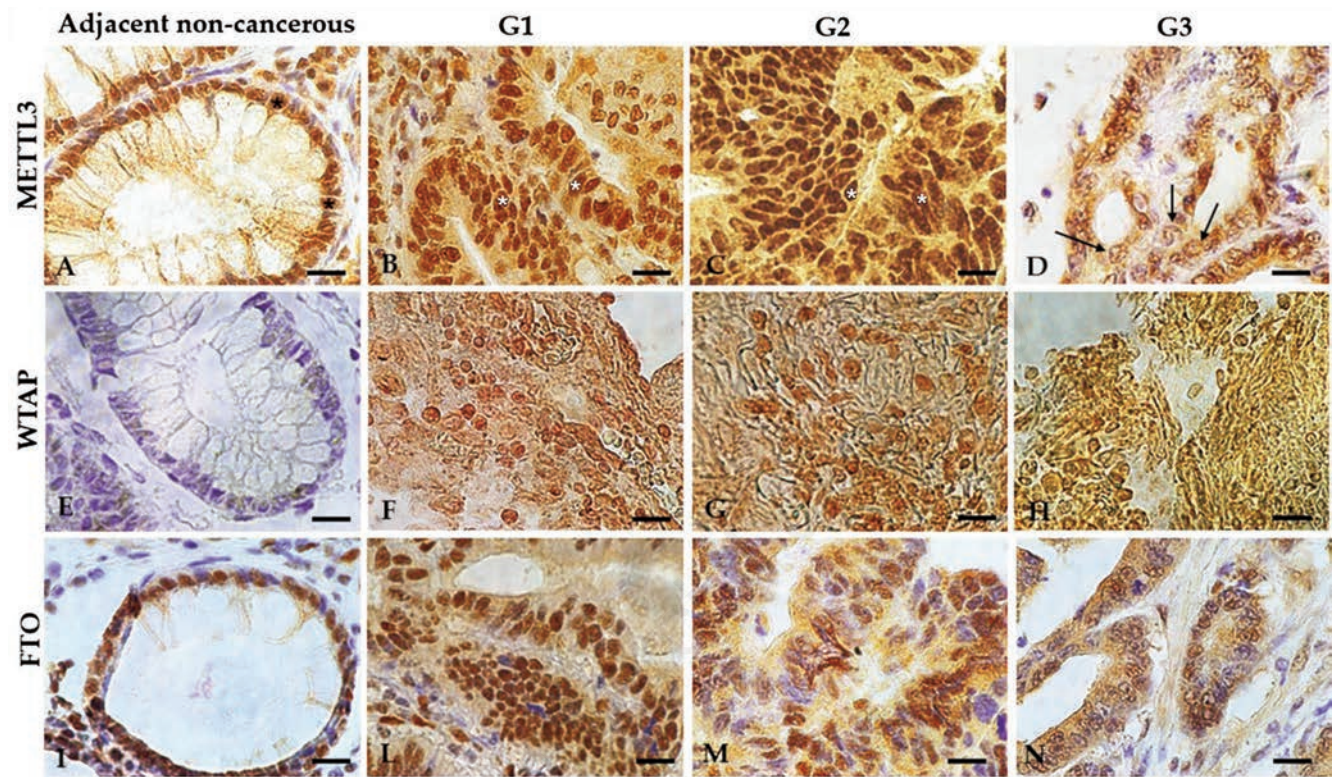


Figure 2. Immunohistochemical staining of METTL3, WTAP, and FTO in adjacent non-cancerous tissue samples and different tumor grades (G1, G2, and G3). **A-D**) METTL3 staining shows that the expression of the protein increases in the G1 remaining quite similar in G2 stages (B,C) compared with normal adjacent tissue (A) and decreases in G3 (D); the protein localization was strongly nuclear (*) and slightly cytoplasmic both in adjacent non-cancerous tissue and G1/ G2 grade and became perinuclear (arrows) and in G3 tissue. **E-H**) WTAP staining highly increases from normal adjacent colon tissue to G1 and declines in advanced stages (G2, G3) exhibiting nuclear and cytoplasmic localization. **I-N**) FTO staining increases its expression in G1 grade (L) and decreases in the advanced stages of G2 and G3 (M,N) changing its localization from nuclear to cytoplasmic. Scale bars: 50 μm .

Table 1. Colon cancer location, TNM staging, and tumor grade of patient's cohort.

Patient ID	Location	TNM	Tumor grade
SR 13150	Colon LT	IIA	G1
TD 2078	Colon RT	IIIB	G2
LB 12460	Colon RT	IIIB	G2
AP 13733	Colon LT	IVA	G3
CR 13456	Colon LT	IIIB	G2
SO 13265	Colon RT	IVB	G1
FG 13820	Colon RT	IIA	G1
MA 11899	Colon LT	IIIC	G3
OG 11994	Colon RT	I	G1
FA 11539	Colon RT	IIIB	G3

LT, left; RT, right.

for METTL3; 1.424 for WTAP; and 1.182 for FTO; indicate that the effect size value was substantial (interpreting Cohen's d key: $d=0.2$ small effect; $d=0.5$ medium effect; $d=0.8$ significant impact, a generally accepted minimum level of power is 0.80). To evaluate if METTL3, WTAP, and FTO RNAs values could be used as prognostic markers we compared their expression in the carcinoma tissue of patients alive after 5 years and in the carcinoma tissue of patients dead after 5 years (Figure 5). The list of alive and dead patients with respective tumor locations, TNM, and tumor grades is reported in Material and Methods (Table 2). In our study no specific location is prevalent; however, most dead patients had an advanced TNM stage and tumor grade.

Even if our cohort is small, the results suggested that only WTAP expression levels were statistically significant in the carcinoma tissue patients alive after 5 years vs carcinoma tissue of patients dead after the same time. Considering the overall data, it is interesting to note that protein levels have a different trend from RNAs levels, protein levels increase from normal adjacent to G1 stage and then decrease in G2 and G3 stages, while RNA, in particular WTAP RNA remains high in high tumor grades, suggesting that high levels of WTAP RNA could be a promising biomarker for poor CRC prognosis. The fact that protein levels decreases while RNA level remains high must be furtherly evaluated. The trends of the other two markers do not change significantly, but we observed a change in the localization of their expression from nuclear to cytoplasmic, this change might be related to a functional change.

Discussion

CRC is a major health concern worldwide, with a high incidence and mortality rate. Biomarkers play a crucial role in detecting, treating, and managing CRC, with ongoing research aimed at identifying effective prognostic and predictive markers to improve patient outcomes.

m6A modification, one of the most frequent and recurrent RNA modifications, has been implicated in various aspects of CRC development and progression.^{32,33} Studies have shown that m6A modification can inhibit CRC's proliferation and metastasis by affecting specific RNA molecules' stability. Furthermore, m6A modification has been associated with lipid metabolism in CRC, suggesting its involvement in metabolic pathways crucial for cancer progression.³⁴

The dysregulation of m6A modification patterns in CRC has been linked to prognosis and tumor microenvironment infiltration, indicating its potential as a prognostic marker and impact on the immune response within the tumor microenvironment.³⁵ m6A-related genes and regulators have been identified as potential therapeutic targets in CRC, emphasizing the importance of understanding the role of m6A modification in this cancer.³⁶ Moreover, m6A modification has been shown to influence the expression of specific onco-

genes and tumor suppressor genes in CRC, further underlining its role in the epigenetic dysregulation observed in this cancer.³⁷

Overall, m6A modification in CRC is a complex and multifaceted process that affects various aspects of cancer biology, including gene expression regulation, tumor microenvironment interactions, and therapeutic responses. Understanding the mechanisms underlying m6A modification in CRC is crucial for developing targeted therapies and improving patient outcomes.

The METTL3 expression has been extensively studied in CRC³⁷ and was found also highly expressed in other cancers such as breast and liver cancer.^{38,39} The work of Lan *et al.*³⁸ reported a significant upregulation of METTL3 in tumor tissues compared to adjacent normal tissues. In the paper of Li *et al.*⁴⁰ was observed a higher expression level of METTL3 in CRC tissues compared with neighboring tissues.

We observed that in our patients, METTL3 protein value increases from adjacent non-tumoral tissue to G1 grade tissue (Figure 3), decreases slightly in G2, and further de-creases in G3. Our findings indicate that METTL3 protein expression is altered in CRC, with consistent evidence pointing toward its upregulation in cancerous tissues,⁴¹ in agreement with the studies.³⁷⁻⁴⁰

WTAP protein expression showed a marked increase between adjacent non-tumoral tissue and G1 grade tissue, its expression then drops slightly in G2 and then again in G3. According to Dong *et al.*,⁴¹ we observed an upregulation of WTAP protein expression in CRC, suggesting that WTAP may play a crucial role in CRC

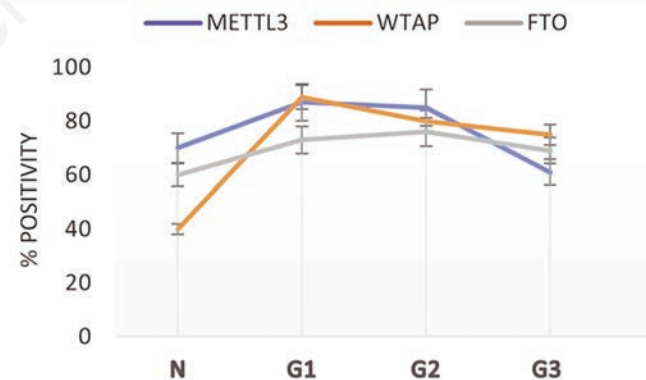


Figure 3. METTL3 WTAP and FTO protein levels were expressed in adjacent non-cancerous and G1-G3 cancerous tissues. m6A protein expression values are the mean \pm SD of 10 counts in triplicate for each sample.

Table 2. Colon cancer location, TNM, and tumor grade in 5-year survived and dead patient.

5-year survived patients	Location	TNM	Tumor grade	Patients dead after 5 years	Location	TNM	Tumor grade
SR 13150/18	Colon LT	IIA	G1	AP 13733/18	Colon LT	IVA	G3
TD 2078/19	Colon RT	IIB	G2	SO 13265/18	Colon RT	IVB	G1
LB 12460/18	Colon RT	IIIB	G2	MA 11899/18	Colon LT	IIIC	G3
CR 13456/18	Colon LT	IIIB	G2	OG 11994/18	Colon RT	I	G1
FG 13820/18	Colon RT	IIA	G1	FA 11539/18	Colon RT	IIIB	G3

LT, left; RT, right.

development. Furthermore, Dai *et al.*⁴² demonstrated that WTAP mediates the N6-methyladenosine modification of PDK4, influencing the malignant behaviors of CRC cells both *in vitro* and *in vivo*. This data indicates that WTAP's involvement in m6A modification contributes to the aggressiveness of CRC. Moreover, Ye *et al.*⁴³ revealed that WTAP activates MAPK signaling through m6A methylation in VEGFA mRNA, mediated by YTHDC1, promoting CRC development. This suggests a mechanistic link between WTAP, m6A modification, and CRC progression. Additionally, Ye *et al.*⁴³ and Zhou *et al.*⁴⁴ both highlighted WTAP as a novel oncogene in CRC through the Wnt signaling pathway, emphasizing its significance in driving CRC pathogenesis.

In a broader context, WTAP has been implicated in various cancers, including CRC, as confirmed by different authors.⁴⁵⁻⁴⁹ Heng *et al.*⁴⁷ further supported the role of ARRB2 in promoting CRC growth through triggering WTAP, suggesting a complex interplay between different factors in CRC progression. Data on WTAP protein expression in our patients resulted in statistically significant differences in normal vs G1 tumor tissue; WTAP expression de-creases in advanced cancer stages, in agreement with the results of Dong *et al.*⁴¹

FTO value increases slightly from adjacent non-tumoral tissue to G1 grade tissue, increases slightly again in G2, and then declines in G3.

The expression of the *FTO* gene in CRC has been a subject of research to understand its role in cancer progression and its potential role as a biomarker or therapeutic target.

In agreement with our results, many studies report that FTO expression is significantly higher in colorectal tumor tissues than in healthy tissues, demonstrating correlations between tumor stage and metastasis.⁵⁰⁻⁵³ However, Liu *et al.*⁵⁴ showed no significant dif-

ference in FTO expression in CRC compared to the one in normal tissue, thus indicating variability in its expression pattern. FTO protein is downregulated in CRC tissues and associated with poor prognosis and increased recurrence.⁵¹ Accordingly, our histochemical results showed an elevated FTO expression in the G1 stage of CRC compared to normal tissue; however, FTO expression decreases in the G2 and G3 stages. Interestingly, protein localization changes from nuclear to cytoplasmic in advanced cancer stages. The complex and unclear role of FTO in CRC could be linked to FTO involvement in CRC progression through various pathways, including the AMPK α 2-FTO-m6A/MYC axis and the Wnt/ β -catenin pathway.^{50,55} Interestingly, the expression of FTO in CRC is associated with the tumor microenvironment, suggesting its involvement in tumor-stroma communication and possibly in early carcinogenic stages.⁵³ The subcellular localization of FTO protein in CRC at different stages has been a matter of significant interest,⁵⁶ demonstrated that the spatial distribution of FTO influences its demethylase activity: cytoplasmic FTO catalyzes the demethylation of both m6A and cap-m6A, while nuclear FTO preferentially demethylates m6A, potentially due to accessibility constraints to the cap-moiety. Furthermore, Ruan *et al.*⁵² provided insights into the downregulation of FTO protein expression mediated by hypoxia. This leads to increased ubiquitin-mediated protein degradation, which may contribute to the observed shift from nuclear to cytoplasmic expression in advanced stages of CRC. Additionally, Gui *et al.*⁵⁷ highlighted the association of FTO with RNA N6-methyladenosine methyltransferase complex and nuclear speckles, indicating its nuclear localization and potential role in the regulation of gene expression. These findings suggest that the dynamic subcellular localization of FTO in CRC may be influenced by hypoxia-induced downregulation, different target sub-

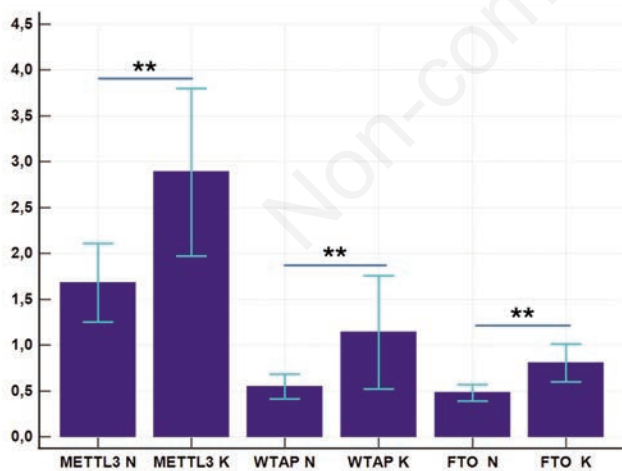


Figure 4. METTL3 WTAP and FTO RNAs expression in patients with different tumor grades (G1, G2, and G3). METTL3, WTAP, and FTO RNAs expression in adjacent non-cancerous (N) and carcinoma (CA) tissue, evaluated by RT-qPCR are significantly different ($p < 0.05$) as calculated by Paired sample t-test (METTL3 N, arithmetic mean=1.6786 SD=0.4281; METTL3 CA, arithmetic mean=2.8873 SD=0.9130, $t=4.484$ $p=0.002$); WTAP N (arithmetic mean=0.5470 SD=0.1388; WTAP CA, arithmetic mean=1.1369 SD=0.6183, $t=3.597$, $p=0.005$); FTO N, (arithmetic mean=0.4472 SD=0.1922; FTO CA, arithmetic mean=0.7342 standard deviation=0.2775; $t=4.132$, $p=0.002$).

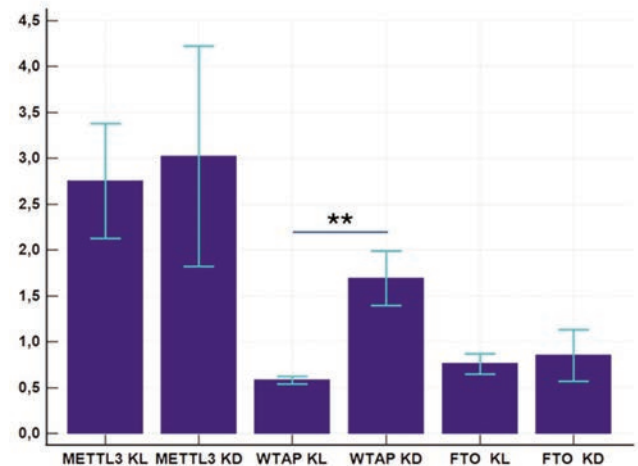


Figure 5. Comparison of METTL3 and WTAP and FTO expression in 5-year-survived (CAL) tumor tissue and dead patients (CAD). Between METTL3 CAL (arithmetic mean=2.7522 SD=0.6247) and METTL3 CAD (arithmetic mean=3.0225 SD=1.1999) no significant difference exists ($t=0.447$, $p=0.6669$). Instead, WTAP expression in CAL (arithmetic mean=0.5814 SD=0.04016) was lower and significantly different ($t=9.447$, $p < 0.0007$) from the value in CAD (arithmetic mean 1.6923 standard deviation = 0.2954). About FTO, no significant difference ($t=0.670$, $p=0.5215$) exists between the two groups (FTO CAL arithmetic mean=0.7588 SD=0.1090; FTO CAD arithmetic mean=0.8497 SD=0.2827).

strates, and its association with nuclear components. All the above provide valuable insights into the mechanistic basis for the observed shift -from nuclear to cytoplasmic expression- in the advanced stages of CRC. To evaluate which among METT3, WTAP, and FTO, had the characteristics of a prognostic biomarker we compared the values of METTL3, WTAP, and FTO RNAs in the tumor tissue of patients alive after 5-year vs those in the tumor tissue of dead patients after the same time. METTL3 level of alive patients was found not significantly different from the value in dead patients, the same was for FTO values.

Instead, in our cohort WTAP RNA expression in the tumor tissue of alive patients was lower than WTAP level in the tumor tissue of dead patients. Thus, we suggest that WTAP's RNA high expression level could be considered a promising biomarker for poor prognosis. The impact of WTAP RNA overexpression on the survival of CRC patients is a matter of clinical significance. WTAP protein expression is upregulated in CRC and negatively associated with tumor differentiation, but no clear relationship between WTAP RNA and patient prognosis has been established until now as stated in the large study of Dong *et al.*⁴¹ The hypothesis may be that protein levels decreases while RNA level remains high due to a sort of suppression of protein expression. The recent findings of Liu *et al.*⁵⁸ suggested that hypoxia reduced WTAP expression in CRC cells by decreasing the ubiquitin-mediated breakdown of WTAP.

In this study we examined the trend of METTL3, WTAP and FTO protein and RNA expression in a cohort of 10 patients: the trend of protein expression was ascending from adjacent non-cancerous tissue to G1 stage (marked difference for WTAP), almost stable between G1-G2 and descending in G3. The RNA expression instead had different behavior, RNAs expression of METTL3, WTAP and FTO in adjacent non-cancerous tissue vs G1 stage tissue was significantly different but analyzing the values in the subgroup of alive patients and dead patients after a time of 5 year, we found that only WTAP RNA value was significantly higher in dead patients who had also the higher tumor grades. The observation of persistence of high WTAP RNA expression while protein expression decrease, let us hypothesize a sort of inhibition of protein expression, but further studies are needed to clarify the mechanism. Considering that our cohort is small, a larger number of patients enrolled in a 5-year follow-up is needed to further confirm the prognostic significance of WTAP in CRC and determine its potential function as a prognostic biomarker for survival in the clinical practice.

References

- International Agency for Research on Cancer, WHO. Global cancer observatory. Accessed 2024. Available from: <https://gco.iarc.fr>
- Zheng S, Schrijvers JJA, Greuter MJW, Kats-Ugurlu G, Lu W, de Bock GH. Effectiveness of colorectal cancer (CRC) screening on all-cause and CRC-specific mortality reduction: A systematic review and meta-analysis. *Cancers (Basel)* 2023;15:1-17.
- Sun H, Meng Q, Shi C, Yang H, Li X, Wu S, et al. Hypoxia-inducible exosomes facilitate liver-tropic premetastatic niche in colorectal cancer. *Hepatology* 2021;74:2633-51.
- Shinagawa T, Tanaka T, Nozawa H, Emoto S, Murono K, Kaneko M, et al. Comparison of the guidelines for colorectal cancer in Japan, the USA, and Europe. *Ann Gastroenterol Surg* 2018;2:6-12.
- Chen K, Collins G, Wang H, Toh JWT. Pathological features and prognostication in colorectal cancer. *Curr Oncol* 2021;28:5356-83.
- Ashouri K, Wong A, Mittal P, Torres-Gonzalez L, Lo JH, et al. Exploring predictive and prognostic biomarkers in colorectal cancer: A comprehensive review. *Cancers (Basel)* 2024;16:2796.
- Alnakli AAA, Mohamedali A, Heng B, Chan C, Shin J-S, Solomon M, et al. Protein prognostic biomarkers in stage II colorectal cancer: Implications for post-operative management. *BJC Rep* 2024;2:13.
- Liu N, Pan T. RNA epigenetics. *Transl Res* 2015;165:28-35.
- Helm M, Motorin Y. Detecting RNA modifications in the epitranscriptome: Predict and validate. *Nat Rev Genet* 2017;18:275-91.
- Gilbert WV, Bell TA, Schaening C. Messenger RNA modifications: Form, distribution, and function. *Science* 2016;352:1408-12.
- Davalos V, Blanco S, Esteller M. SnapShot: Messenger RNA modifications. *Cell* 2018;174:498-498.e1.
- Boccaletto P, Stefaniak F, Ray A, Cappannini A, Mukherjee S, Purta E, et al. MODOMICS: A database of RNA modification pathways. *Nucleic Acids Res* 2022;50:D231-5.
- Dai D, Wang H, Zhu L, Jin H, Wang X. N6-methyladenosine links RNA metabolism to cancer progression. *Cell Death Dis* 2018;9:124.
- Zhao BS, Roundtree IA, He C. Post-transcriptional gene regulation by mRNA modifications. *Nat Rev Mol Cell Biol* 2017;18:31-42.
- Wang S, Sun C, Li J, Zhang E, Ma Z, Xu W, et al. Roles of RNA methylation by means of N (6)-methyladenosine (m6A) in human cancers. *Cancer Lett* 2017;408:112-20.
- Nombela P, Miguel-López B, Blanco S. The role of m6A, m5C and ΨRNA modifications in cancer: Novel therapeutic opportunities. *Mol Cancer* 2021;20:1-30.
- Wu F, Cheng W, Zhao F, Tang M, Diao Y, Xu R. Association of N6-methyladenosine with viruses and related diseases. *Virology* 2019;16:133.
- Liu ZX, Li LM, Sun HL, Liu SM. Link between m6A modification and cancers. *Front Bioeng Biotechnol* 2018;6:89.
- Zaccara S, Ries RJ, Jaffrey SR. Reading, writing and erasing mRNA methylation. *Nat Rev Mol Cell Biol* 2019;20:608-24.
- Frye M, Harada BT, Behm M, He C. RNA modifications modulate gene expression during development. *Science* 2018;361:1346-9.
- Shi H, Wei J, He C. Where, when, and how: Context-dependent functions of RNA methylation writers, readers, and erasers. *Mol Cell* 2019;74:640-50.
- Hamilton SR, Bosman FT, Boffetta P, Theise ND. Carcinoma of the colon and rectum. In: Bosman FT, Carneiro F, Hruban RH, Theise ND, Editors, WHO Classification of tumours of the digestive system. Lyon, IARC Press; 2010. pp. 134-46.
- Compton C, Fenoglio-Preiser CM, Pettigrew N, Fielding LP. American joint committee on cancer prognostic factors consensus conference: Colorectal working group. *Cancer* 2000;88:1739-57.
- Compton CC. Key issues in reporting common cancer specimens: Problems in pathologic staging of colon cancer. *Arch Pathol Lab Med* 2006;130:318-24.
- Di Emidio G, Placidi M, Rea F, Rossi G, Falone S, Cristiano L, et al. Methylglyoxal-dependent glycation stress and deregulation of SIRT1 functional network in the ovary of PCOS mice. *Cells* 2020;14:209.
- Bossù M, Matassa R, Relucenti M, Iaculli F, Salucci A, Di Giorgio G, et al. Morpho-chemical observations of human deciduous teeth enamel in response to biomimetic toothpastes treatment. *Materials (Basel)* 2020;13:1803.
- Relucenti M, Heyn R, Petruzzello L, Pugliese G, Taurino M, Familiari G. Detecting microcalcifications in atherosclerotic plaques by a simple trichromic staining method for epoxy-embedded carotid endarterectomies. *Eur J Histochem* 2010;54:e33.
- Relucenti M, Heyn R, Correr S, Familiari G. Cumulus oophorus extracellular matrix in the human oocyte: A role for adhesive proteins. *Int J Anat Embryol* 2005;110:219-24.
- Relucenti M, Francescangeli F, De Angelis ML, D'Andrea V, Miglietta S, Pillozzi E, et al. The ultrastructural analysis of human colorectal cancer stem cell-derived spheroids and their mouse xenograft shows that the same cell types have different

- ratios. *Biology (Basel)* 2021;10:929.
30. Relucenti M, Francescangeli F, De Angelis ML, D'Andrea V, Miglietta S, Donfrancesco O, et al. A different exosome secretion pattern characterizes patient-derived colorectal cancer multicellular spheroids and their mouse xenografts. *Biology (Basel)* 2022;11:1427.
 31. Sawilowsky SS. New effect size rules of thumb. *J Mod Appl Stat Methods* 2009;8:597-9.
 32. Yi D, Xu F, Wang R, Jiang C, Qin J, Lee Y, Shi X, Sang J et al. Deciphering the map of METTL14-mediated lncRNA m6A modification at the transcriptome-wide level in breast cancer. *J Clin Lab Anal* 2022;36:e24754.
 33. Xu X, Huang J, Ocansey DKW, Xia Y, Zhao Z, Xu Z, et al. The emerging clinical application of m6A RNA modification in inflammatory bowel disease and its associated colorectal cancer. *J Inflamm Res* 2021;14:3289-306.
 34. Guo W, Zhang C, Feng P, Li M, Wang X, Xia Y, et al. M6A methylation of DEGS2, a key ceramide-synthesizing enzyme, is involved in colorectal cancer progression through ceramide synthesis. *Oncogene* 2021;40:5913-24.
 35. Yue Q, Zhang Y, Wang F, Cao F, Bai J, Duan X. Characterization of m6A methylation modification patterns in colorectal cancer determines prognosis and tumor microenvironment infiltration. *J Immunol Res* 2022;2022:8766735.
 36. Ozato Y, Hara T, Meng S, Sato H, Tatekawa S, Uemura M, et al. RNA methylation in inflammatory bowel disease. *Cancer Sci* 2024;115:723-33.
 37. Zhang Z, Zhang X. Identification of m6A-related biomarkers associated with prognosis of colorectal cancer. *Med Sci Monit* 2021;27:e932370.
 38. Lan Q, Liu PY, Haase J, Bell JL, Hüttelmaier S, Liu T. The critical role of RNA m6A methylation in cancer. *Cancer Res* 2019;79:1285-92.
 39. Pu J, Wang J, Qin Z, Wang A, Zhang Y, Wu X, et al. IGF2BP2 promotes liver cancer growth through an m6A-FEN1-dependent mechanism. *Front Oncol* 2020;10:578816.
 40. Li H, Liu Z, Wang H. Expression and clinical significance of METTL3 in colorectal cancer. *Medicine (Baltimore)* 2023;102:e34658.
 41. Dong X, Wang Y, Tang CH, Huang BF, Du Z, Wang Q, et al. Upregulated WTAP expression in colorectal cancer correlates with tumor site and differentiation. *PLoS One* 2022;17:e0263749.
 42. Dai X, Chen K, Xie Y. WTAP mediated the N6-methyladenosine modification of PDK4 to regulate the malignant behaviors of colorectal cancer cells in vitro and in vivo. *Curr Med Chem* 2023;30:3368-81.
 43. Ye M, Chen J, Yu P, Hu C, Wang B, Bao J, et al. WTAP activates MAPK signaling through m6A methylation in VEGFA mRNA mediated by YTHDC1 to promote colorectal cancer development. *FASEB J* 2023;37:e23090.
 44. Zhou Z, Lv J, Yu H, Han J, Yang X, Feng D, et al. Mechanism of RNA modification N6-methyladenosine in human cancer. *Mol Cancer* 2020;19:104.
 45. Fang Z, Hu Y, Hu J, Huang Y, Zheng S, Guo C. The crucial roles of N6-methyladenosine (m6A) modification in the carcinogenesis and progression of colorectal cancer. *Cell Biosci* 2021;11:72.
 46. Liu W, Gao X, Chen X, Zhao N, Sun Y, Zou Y, et al. Mir-139-5p loss-mediated WTAP activation contributes to hepatocellular carcinoma progression by promoting the epithelial to mesenchymal transition. *Front Oncol* 2021;11:611544.
 47. Heng L, Lin Z, Ye Y, Luo R, Zeng L. ARRB2 promotes colorectal cancer growth through triggering WTAP. *Acta Biochim Biophys* 2020;53:85-93.
 48. Xie W, Wei L, Guo J, Guo H, Song X, Sheng X. Physiological functions of Wilms' tumor 1-associating protein and its role in tumorigenesis. *J Cell Biochem* 2019;120:10884-92.
 49. Lei J, Fan Y, Yan C, Jiamaliding Y, Tang Y, Zhou J, et al. Comprehensive analysis about prognostic and immunological role of WTAP in pan-cancer. *Front Genet* 2022;13:1007696.
 50. Muinelo-Romay L, Vázquez-Martín C, Villar-Portela S, Cuevas E, Gil-Martín E, Fernández-Briera A. Expression and enzyme activity of α (1,6) fucosyltransferase in human colorectal cancer. *Int J Cancer* 2008;123:641-6.
 51. Yue C, Chen J, Li Z, Li L, Chen J, Guo Y. MicroRNA-96 promotes occurrence and progression of colorectal cancer via regulation of the AMPK α 2-FTO-m6A/MYC axis. *J Exp Clin Cancer Res* 2020;39:240.
 52. Ruan D, Li T, Wang Y, Meng Q, Li Y, Yu K, et al. FTO down-regulation mediated by hypoxia facilitates colorectal cancer metastasis. *Oncogene* 2021;40:5168-81.
 53. Landskron-Ramos G, Domínguez-Beltrando A, Zambra-Rojas M, Sanguinetti A, Vasquez G, Fuente M, et al. Abstract 1251: Novel potential role of m6A-demethylase FTO (fat mass and obesity) protein in colorectal cancer. *Cancer Res* 2023;83:1251.
 54. Liu X, Liu L, Dong Z, Li J, Yu Y, Chen X, et al. Expression patterns and prognostic value of m6A-related genes in colorectal cancer. *Am J Transl Res* 2019;11:3972-91.
 55. Li J, Li S, Xing X, Liu N, Lai S, Liao D, Li J. FTO-mediated ZNF687 accelerates tumor growth, metastasis, and angiogenesis in colorectal cancer through the Wnt/ β -catenin pathway. *Biotechnol Appl Biochem* 2024;71:245-55.
 56. Relier S, Rivals E, David A. The multifaceted functions of the fat mass and obesity-associated protein (FTO) in normal and cancer cells. *RNA Biol* 2022;19:132-42.
 57. Gui S, Wang Q, Bao L, He X, Wang Z, Liu L, et al. Effects of *Helicobacter pylori* on the expression of the FTO gene and its biological role in gastric cancer. *Oncol Lett* 2023;25:143.
 58. Liu QZ, Zhang N, Chen JY, Zhou MJ, Zhou DH, Chen Z, et al. WTAP-induced N6-methyladenosine of PD-L1 blocked T-cell-mediated antitumor activity under hypoxia in colorectal cancer. *Cancer Sci* 2024;115:1749-62.

Received: 15 August 2024. Accepted: 18 November 2024.

This work is licensed under a Creative Commons Attribution-NonCommercial 4.0 International License (CC BY-NC 4.0).

©Copyright: the Author(s), 2024

Licensee PAGEPress, Italy

European Journal of Histochemistry 2024; 68:4145

doi:10.4081/ejh.2024.4145

Publisher's note: all claims expressed in this article are solely those of the authors and do not necessarily represent those of their affiliated organizations, or those of the publisher, the editors and the reviewers. Any product that may be evaluated in this article or claim that may be made by its manufacturer is not guaranteed or endorsed by the publisher.